

Femtosecond Fluorescence Anisotropy Studies of Excited-State Intramolecular Double-Proton Transfer in [2,2'-bipyridyl]-3,3'-diol in Solution

P. Toele, H. Zhang, and M. Glasbeek*

Laboratory for Physical Chemistry, University of Amsterdam, Nieuwe Achtergracht 129, 1018 WS Amsterdam, The Netherlands

Received: September 10, 2001; In Final Form: January 14, 2002

For [2,2'-bipyridyl]-3,3'-diol (BP(OH)₂), dissolved in aprotic solvents, the time dependence of the fluorescence anisotropy has been studied using the femtosecond fluorescence *up-conversion* technique. A fast fluorescence anisotropy decay, with a characteristic time of ~ 350 fs, is observed when detection is at 460 nm, i.e., near the blue edge of the BP(OH)₂ broad-band emission. It is discussed that the fast decay is typical of emission from the “di-enol” excited Franck–Condon state for which the lifetime is limited by the first steps of a branched excited-state double double-proton-transfer process. The branched reaction includes concerted and consecutive double-proton-transfer. The fast decay of the “di-enol” excited state into “mono-keto” and “di-keto” excited states is indicative of a (quasi-)barrierless reaction. To explain that the rapid (~ 350 fs) initial decay is manifested in the fluorescence anisotropy, it is conjectured that the electronic wave function characteristic of the emissive state is a reaction-coordinate dependent admixture of diabatic wave functions, these functions being characteristic of the “enol”- and “keto”-tautomers. The progress of the double-proton-transfer reaction is accompanied by a change of the admixture of the excited-state tautomer wave functions and in this way gives rise to a rapid decay in the fluorescence anisotropy. The fluorescence anisotropy of BP(OH)₂ furthermore includes two slower decay components. These components, with time constants of a few tens of picoseconds, are related to the second step of the consecutive double proton-transfer kinetics (~ 10 ps) and the rotational diffusion motions of the solute in the liquid (20–40 ps).

1. Introduction

Photoinduced excited-state intramolecular proton transfer (ESIPT) reactions have attracted widespread interest.¹ Single and multiple (concerted and consecutive) proton transfer reactions have been studied using femto- and picosecond spectroscopy.² In this paper, we focus on the double-proton transfer in photoexcited [2,2'-bipyridyl]-3,3'-diol (BP(OH)₂, Figure 1). BP(OH)₂ and its derivatives have potential as laser dyes³ and solar energy collectors.⁴ Excited-state double-proton transfer (ESDPT) in BP(OH)₂ has been extensively studied, both experimentally^{5–11} and theoretically.^{12,13} On the basis of the very large Stokes shift of the emission band maximum with respect to the absorption band maximum (of about $10\,000\text{ cm}^{-1}$) and the insensitivity of the positions of the absorption and emission band maxima to the solvent polarity, the fluorescent state of BP(OH)₂ has been attributed to the “di-keto” tautomer,¹⁴ in which the two hydroxyl-group protons are displaced toward the pyridyl-ring nitrogen atoms. Electrooptical experiments^{6,7} and quantum mechanical calculations provided additional support for ESDPT in BP(OH)₂.^{12,13}

Recently, several studies have provided information concerning the dynamics of the excited-state double-proton transfer in BP(OH)₂.^{8–11,15} From femtosecond fluorescence up-conversion^{7–10} and transient absorption¹⁵ measurements, it was concluded that ESDPT in BP(OH)₂ is branched, i.e., the process can be concerted (one-step) as well as sequential (two-step). The concerted reaction is ultrafast with a typical time of about 100 fs or less; the consecutive reaction, with an ultrafast first step

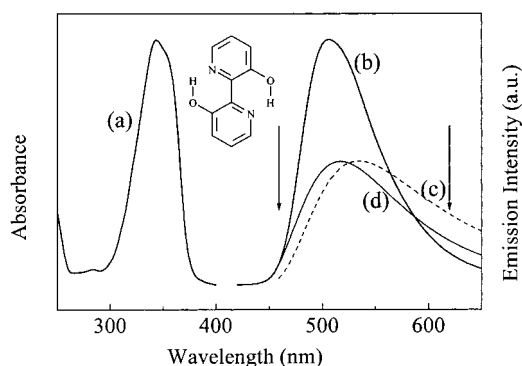


Figure 1. Absorption (a) and emission (b) spectra of BP(OH)₂ dissolved in cyclohexane. Arrows indicate positions of the detection wavelengths (460 and 620 nm) used in the fluorescence up-conversion experiments. Reconstructed emission spectra for “mono-keto” (c) and “di-keto” (d) tautomers of BP(OH)₂ in cyclohexane in consecutive proton transfer reaction at 10 ps after pulsed excitation at 310 nm. In the figure the intensity scale of spectra (c) and (d) is not related to that of (b). Structure of BP(OH)₂ is given as inset.

(approximately 100 fs or less) and a second step of ~ 10 ps, is solvent and excitation wavelength dependent. Stretching and bending skeletal modes within the BP(OH)₂ molecule have been considered as promoting modes for the one-step and two-step double-proton-transfer reactions, respectively.⁹

For BP(OH)₂, the branching of the excited-state tautomeric reactions reflects a highly unsymmetrical excited-state potential energy surface in reaction-coordinate space (analogous to that recently reported for chrysazin¹⁶ and 10-hydroxybenzo[*h*]-quinoline¹⁷). Due to the asymmetric shape of the excited-state potential energy surface, we may expect that the electronic part

* Corresponding author. E-mail: glasbeek@science.uva.nl. FAX: +31 20 5256994.

of the molecular wave function varies significantly during the ESDPT reaction. It is thus conceivable that the proton-transfer reactions of photoexcited BP(OH)₂ give rise to ultrafast temporal components in the fluorescence anisotropy.^{18–20} Sensitive detection of these effects should be feasible utilizing the femtosecond fluorescence up-conversion technique, provided of course the electronic relaxation involves directional changes in the electronic transition dipole moment and the dynamics associated with these changes is much faster than the tumbling motions of the probed molecules.²¹

In this paper, we investigate the time-dependence of the fluorescence anisotropy of BP(OH)₂ in aprotic solvents, the solvents being cyclohexane and acetonitrile. The temporal dependence of the fluorescence anisotropy detected at the trailing edge of the blue wing emission of BP(OH)₂, near 460 nm, reveals the existence of an ultrafast decay component with a typical time of ~350 fs. The new component is discussed to originate from the initially excited “di-enol” excited Franck–Condon state. Since the lifetime of this state determines the double-proton-transfer rate of BP(OH)₂, the result represents the first measurement of the proton transfer time in the “dienol”-to-“keto” reaction in photoexcited BP(OH)₂ in liquid solution.

2. Experimental Section

The compound [2,2'-bipyridyl]-3,3'-diol was purchased from Aldrich and used as received. The solvents, anhydrous cyclohexane (Fluka) and acetonitrile (Fluka), were of spectrograde quality. BP(OH)₂ was dissolved in a concentration of about 10^{−4} mol/L.

Steady-state absorption spectra were recorded by means of a Shimadzu UV-240 spectrophotometer. The steady-state fluorescence spectra were measured using the emission spectrometer described previously.²² The emission spectra were corrected for the wavelength-dependent sensitivity of the monochromator-photomultiplier detection system.

Femtosecond fluorescence up-conversion experiments were performed using the setup described previously.¹¹ A mode-locked Tsunami Ti:sapphire laser was optically pumped by a Spectra-Physics Millennia X Nd:YVO₄ CW diode-laser, to produce pulses, at a wavelength of 800 nm, with a duration of about 60 fs and a repetition rate of 82 MHz. Amplification was by means of a Quantronix regenerative amplifier system (RGA), which generated pulses, with an energy of approximately 500 μJ/pulse and a repetition rate of 1 kHz. The amplified pulses were split into two beams, one beam served to pump an optical parametric amplifier system (TOPAS Light Conversion Ltd.). The wavelength-tunable laser pulses from the TOPAS were used to optically excite the sample. Typically, in the up-conversion experiments the excitation wavelength for BP(OH)₂ could be varied between 310 and 380 nm; in these experiments the duration of the excitation pulses was about 150 fs, whereas the pulse energy was about 1 μJ. Laser fluence was kept low enough to ensure that the fluorescence intensity was linear dependent on the laser intensity. The solution was contained in a quartz cell of 1 mm thickness. The cell was attached to a sample holder that was driven electrically back and forth perpendicular to the excitation direction to prevent heating of the sample. A 420 nm cutoff filter immediately behind the sample prevented that scattered laser and/or Raman light was included in the detection pathway. The second laser beam, the gating beam, was first led through an optical delay line. Generation of the up-conversion signal was accomplished by wave mixing of the gating beam with the laser-induced fluorescence in a 1 mm BBO crystal (type I phase matching conditions). The up-converted

fluorescence light was led through an UG 11 band-pass filter and focused onto the entrance slit of a Zeiss M4 prism monochromator outfitted with an EMI 9863 QB/350 photomultiplier. It was checked that reliable detection of the up-conversion signal intensity was possible for wavelengths of 460 nm and higher. Detection of the output signal from the photomultiplier was by means of lock-in detection. The experiments were restricted to the measurement of fluorescence transients. The data were digitally stored and analyzed by a personal computer. From the measured transients the time-resolved emission spectra were obtained applying the spectral reconstruction method (Section 3). In this method time zero is well defined and, unlike in the direct measurement of time-resolved emission spectra, additional correction for group velocity dispersion is not necessary. The system response time as obtained from the fwhm of the cross-correlation signal of the gate- and excitation-beams is 300 ± 20 fs.

An optical polarizer in the excitation pathway was used to control the polarization direction of the excitation pulses relative to the vertically polarized gating-beam pulses. Measurements under magic angle conditions (with the laser-excitation polarization at an angle of 54.7° relative to the vertically polarized gating beam) were also performed. In these experiments, the effects of rotational diffusion motions of the solute molecules in the liquid on the fluorescence depolarization are eliminated.²¹

A second laser system, outfitted with a time-correlated single-photon-counting (TCSPC) detection system, was used for the measurement of the fluorescence transients in a time span 15 ps–5 ns. Details of the setup are given elsewhere.²² Extension of the time window to the picosecond-nanosecond range is essential for the calibration of the intensities of the transients obtained in the femtosecond measurements. Photoexcitation was by means of picosecond pulses from a mode-locked Ar⁺-ion laser (Coherent, Innova 200–15) synchronously pumping a dye laser (Coherent, 702–3) with a cavity dumper (Coherent, 7200). The cavity-dumped dye laser generated laser pulses with a duration of about 1 ps (fwhm autocorrelation trace), an energy of about 25 nJ/pulse and a repetition rate of 3.7 MHz. These pulses were frequency doubled in a 6 mm BBO crystal, yielding pulses at a wavelength of 322 nm to photoexcite the sample. The fluorescence emitted from the sample in a direction perpendicular to the excitation beam was focused onto the entrance slit of a monochromator outfitted with a multichannel plate photodetector. A linear polarizer was inserted in the detection pathway to detect the intensity of the parallel and perpendicular polarized transients and at magic angle conditions. The instrumental response time was about 17 ps (fwhm).

3. Results

Figure 1 shows the steady-state absorption and emission spectra of BP(OH)₂. The S₁ ← S₀ absorption band has its maximum near 340 nm ($\epsilon = 1.7 \times 10^4 \text{ M}^{-1} \text{ cm}^{-1}$) in agreement with previous measurements.⁵ Semiempirical calculations indicated that the S₁ ← S₀ excitation involves a π - π^* transition.⁵ The emission maximum is near 510 nm, the emission quantum yield being $\eta_f = 0.22$. The emission is characteristic of the “di-keto” tautomer.²³ Emission due to the directly excited “di-enol” tautomer has so far not been reported.

Previously we presented femtosecond fluorescence up-conversion transients for BP(OH)₂, obtained under magic angle conditions for a series of detection wavelengths.^{7–10} From the results, the short-time emission spectra of BP(OH)₂ could be reconstructed. At early times ($t < 10$ ps), the existence of two emission bands could be inferred: one band, with a maximum

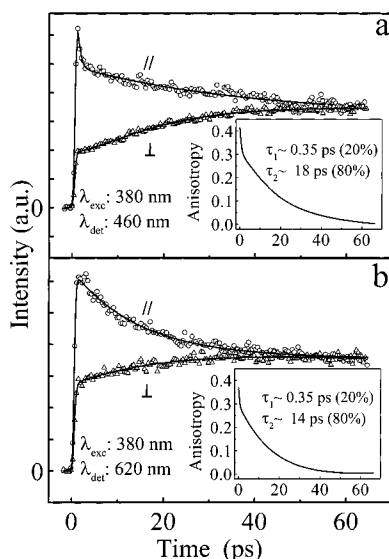


Figure 2. Polarized femtosecond fluorescence up-conversion transients of BP(OH)₂, dissolved in cyclohexane, for excitation at 380 nm and detection at (a) 460 nm, and at (b) 620 nm. Open circles and triangles: experimental data points, polarization is as indicated; solid lines: best-fits to multiexponential functions. Insets show the corresponding fluorescence anisotropy decays

near 568 nm, consisting of a superposition of the short-living “mono-keto” intermediate and the “di-keto” emission, and a second band, with its maximum near 510 nm, characteristic of solely the “di-keto” product. Results of AM1 calculations suggested that the energy corresponding to the electronic ground state of the “mono-keto” tautomer lies well above that for the “di-keto” form.¹² This explains why the emission of the former is shifted to the red with respect to the steady-state emission due to the “di-keto” form. In cyclohexane, the lifetime of the 568 nm band is approximately 10 ps. The emission due to the relaxed “di-keto” excited state, at 510 nm, has a lifetime of 3.0 ns. In Figure 1 we have included the reconstructed “mono-” and “di-keto” bands, (c) and (d), respectively, at 10 ps after the pulsed excitation of BP(OH)₂ (in cyclohexane).

For the time-resolved polarized emission transients of BP(OH)₂ presented here, the excitation wavelengths ranged from 380 nm (close to the 0–0 absorption) up to 310 nm (the vibrational excess energy being about 6000 cm⁻¹). Detection wavelengths were chosen between 460 and 620 nm (see arrows in Figure 1). At 460 nm the emission is mainly due to the “di-keto” form, at 620 nm the emission is composed of “mono-keto” and “di-keto” tautomer contributions.⁸

Figure 2 shows a few representative fluorescence up-conversion transients of BP(OH)₂, in cyclohexane, for parallel and perpendicular polarized detection with respect to the polarization of the 380 nm excitation pulses, when detection is at 460 nm (a) and 620 nm (b), respectively. The experimental transients were fitted to a sum of exponential functions convoluted with the system response function. The system response function (see also Figure 4) was the sum-frequency signal of the excitation light at 380 nm and the 800 nm gate beam. Transients with a 10 ps time window were normalized using the 70 ps-window transients; the latter were normalized to the picosecond fluorescence transients obtained with time-correlated single photon counting detection, using the procedure described previously.¹¹

We now define $I_{||}(t)$ and $I_{\perp}(t)$ as the time-dependent parallel- and perpendicular-polarized fluorescence intensities characteristic of BP(OH)₂. The experimental polarized transients were

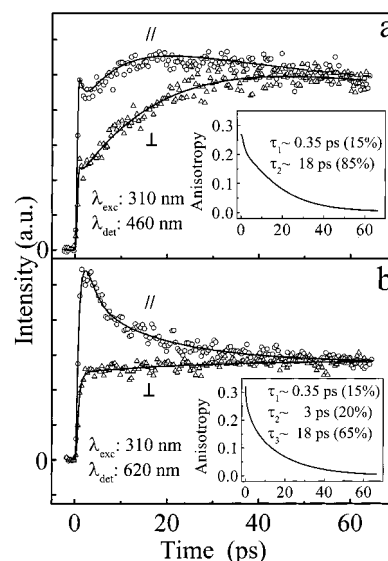


Figure 3. Polarized femtosecond fluorescence up-conversion transients of BP(OH)₂, dissolved in cyclohexane, for excitation at 310 nm and detection at (a) 460 nm, and at (b) 620 nm. Open circles and triangles: experimental data points, polarization is as indicated; solid lines: best-fits to multiexponential functions. Insets show the corresponding fluorescence anisotropy decays.

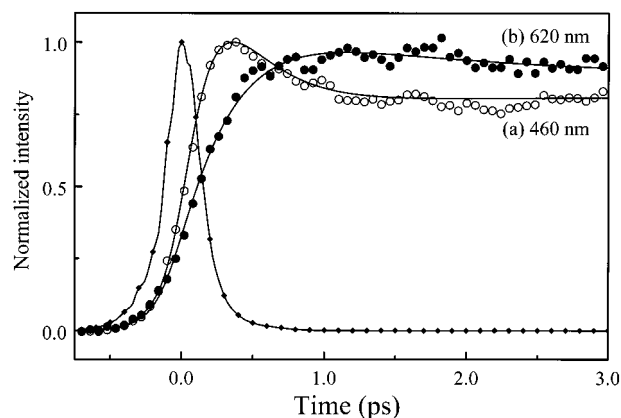


Figure 4. Initial part of fluorescence up-conversion transients of BP(OH)₂ (time window: 3 ps), dissolved in cyclohexane, for excitation at 380 nm and detection, under magic angle conditions, at (a) 460 nm and (b) 620 nm. The system response function near $t = 0$, as obtained from the cross correlation signal of the fundamental and frequency-doubled beams, is included.

fitted to a sum of four exponential terms (this sum being representative of either $I_{||}(t)$ or $I_{\perp}(t)$) convoluted with the system response function using a nonlinear least-squares-fitting analysis. The amplitudes and the rate constants of the four exponential terms were adjusted until best-fit functions for $I_{||}(t)$ and $I_{\perp}(t)$ were obtained. Optimal fit quality was judged by minimization of χ^2 and visual inspection of the residual plots. Best-fit curves are plotted in Figure 3 as solid lines.

The transients detected at 460 nm showed an ultrafast rise component. The convolution of the response function with an artificial function with an ultrafast rise shorter than ~ 150 fs followed by a long exponential decay (> 1 ns) renders a rising curve that matches the observed rise components of Figure 2 a. It follows that the resolution of the characteristic times of the initial rise components is limited to ~ 150 fs. Table 1 summarizes the results of the best-fit parameters for the polarized transients of the “di-keto” tautomer. Likewise, the transients detected at 620 nm (Figure 2 b) were fitted to a multiexponential function convoluted with the system response

TABLE 1: Characteristic Times of Exponential Terms^a in the Best-fit Functions $I_{||}(t)$ and $I_{\perp}(t)$ for the Polarized Fluorescence Up-Conversion Transients of BP(OH)₂ in Cyclohexane

λ_{det} (nm)	pol	excitation: 380 nm			excitation: 310 nm			
		τ_1 (ps)	τ_2 (ps)	τ_3 (ns)	τ_1 (ps)	τ_2 (ps)	τ_3 (ps)	τ_4 (ns)
460		0.35 (0.4)	40 (0.2)	3.0 (0.4)	~0.5 (0.2)	6 (-0.3)	40 (0.2)	3.0 (0.6)
460	⊥		12 (-0.4)	3.0 (1.0)	0.35 (0.1)	14 (-0.8)		3.0 (0.9)
460	$r(t) = 0.41(0.2\exp(-t/0.35) + 0.8\exp(-t/18))$				$r(t) = 0.27(0.2\exp(-t/0.35) + 0.8\exp(-t/18))$			
620		0.35 (-0.9)	12 (0.4)	3.0 (0.6)	0.35 (-0.9)	7 (0.4)	40 (0.2)	3.0 (0.4)
620	⊥	0.35 (-0.6)	14 (-0.3)	3.0 (1.0)	0.35 (-0.4)	40 (-0.2)		3.0
620	$r(t) = 0.37(0.2\exp(-t/0.35) + 0.8\exp(-t/14))$				$r(t) = 0.32(0.2\exp(-t/0.35) + 0.2\exp(-t/3) + 0.6\exp(-t/18))$			

^a Relative weights are given in brackets**TABLE 2: Characteristic Times of Exponential Terms^a in the Best-Fit Functions $I_{||}(t)$ and $I_{\perp}(t)$ for the Polarized Fluorescence Up-Conversion Transients of BP(OH)₂ in Acetonitrile**

λ_{det} (nm)	pol	excitation: 360 nm			excitation: 310 nm			
		τ_1 (ps)	τ_2 (ps)	τ_3 (ns)	τ_1 (ps)	τ_2 (ps)	τ_3 (ps)	τ_4 (ns)
460		~0.3(0.2)	22 (0.2)	1.0(0.6)	~0.4(0.3)	7 (-0.3)	48 (0.2)	1.0 (0.6)
460	⊥	~0.3(0.1)	8 (-0.5)	1.0(0.9)	~0.4 (0.1)	16 (-0.8)		1.0 (0.9)
460	$r(t) = 0.35(0.2\exp(-t/0.3) + 0.4\exp(-t/7) + 0.05\exp(-t/17))$				$r(t) = 0.30(0.1\exp(-t/0.25) + 0.5\exp(-t/11) + 0.4\exp(-t/18))$			
620		~0.2(-0.85)	11 (0.4)	1.0 (0.6)	~0.2 (-0.9)	5 (0.5)		1.0 (0.5)
620	⊥	~0.2 (-0.6)	11 (-0.4)	1.0 (1.0)	~0.2 (-0.6)	9 (-0.4)		1.0 (1.0)
620	$r(t) = 0.40(0.20\exp(-t/0.3) + 0.65\exp(-t/10) + 0.15\exp(-t/20))$				$r(t) = 0.4(0.25\exp(-t/0.25) + 0.7\exp(-t/9) + 0.05\exp(-t/20))$			

^a Relative weights are given in brackets.

function. It is of interest to note that special attention was paid to the time resolution of the rise component. Careful inspection of the transients obtained when applying a time window of 3 ps or less (not shown, see however also the magic angle results of Figure 4), revealed that now the rise component can be time-resolved, the characteristic rise time being ~ 350 fs.

The best-fit functions for $I_{||}(t)$ and $I_{\perp}(t)$ were used to calculate the time dependence of the fluorescence anisotropy, $r(t)$, where

$$r(t) = \frac{I_{||}(t) - I_{\perp}(t)}{I_{||}(t) + 2I_{\perp}(t)} \quad (1)$$

For the signals detected at 460 and 620 nm the plots for $r(t)$ are included in Figure 2 (insets). The respective functional forms are included in Table 1. The fluorescence anisotropy of the “460 nm” emission resulting from the best-fit curves (Figure 2a) has an initial value of about 0.4. The anisotropy shows a biexponential decay, with characteristic times of about 0.35 ps (20%) and 18 ps (80%).

In Figure 3, we present typical fluorescence up-conversion transients obtained when excitation is at 310 nm. Figure 3a illustrates that for the parallel-polarized “460 nm” (“di-keto” tautomer) transient, the initial rise is followed by a sharp initial decay, followed by a rise. The latter rise was not observed when excitation is at 380 nm. The presence of this rise causes that the sharp initial decay becomes very prominent in the parallel-polarized “460 nm” fluorescence transient. The solid curves in Figure 3a represent the plots of the convoluted best-fit functions; the corresponding time constants and relative weights of the best-fit exponential components are included in Table 1. From the best-fit functions the temporal dependence of the fluorescence anisotropy is obtained as plotted in the insert in Figure 3a. The fluorescence anisotropy has an initial value of almost ~ 0.3 . The time dependence of the anisotropy of the “460 nm” emission fits a biexponential function, with typical times of 0.35 ps (20%) and 18 ps (80%).

Fluorescence up-conversion transients when excitation is at 310 nm and detection is at 620 nm are presented in Figure 3b. The time constants and relative weights of the best-fit expo-

nential rise and decay components are given in Table 1. The solid curves in Figure 3b show the best-fit multiexponential functions convoluted with the system response function. From the fittings the anisotropy curve is as displayed in the insert in Figure 3b.

For BP(OH)₂ dissolved in acetonitrile similar experiments were performed. The quality of the fluorescence up-conversion transients and the transients measured with the picosecond time-correlated single photon counting setup for BP(OH)₂ in acetonitrile was similar to that presented in Figures 2 and 3, and for this reason are not reproduced here. Table 2 summarizes the results for the time constants and the relative amplitudes of the various components.

4. Discussion

In previous investigations of BP(OH)₂, it had already been concluded that the absorption near 340 nm primarily involves a $\pi-\pi^*$ excitation of the molecule in its “di-enol” form;⁵ the steady-state emission with a maximum near 510 nm could be attributed to the “di-keto” tautomer, formed after a double-proton transfer in the excited state.⁵ Subpicosecond time-resolved measurements revealed that the double-proton transfer for BP(OH)₂ involves branched concerted and consecutive reactions.⁸ The results of the present paper provide further details about these excited-state processes.

In discussing the temporal behavior of the transients of Figure 2a, we recall that the “460 nm” fluorescence is predominantly due to the “di-keto” tautomer. Apart from the ultrafast formation of this tautomer in the concerted process, it has previously been discussed that this tautomer is also formed (on a time scale of 10 ps) from the “mono-keto” intermediate.⁸ For the parallel-polarized fluorescence transient (Figure 2a), however, a new hitherto unobserved ultrafast fast decay (~ 350 fs) component is observed in addition to the longer decay components (40 ps and 3 ns). The ~ 350 fs decay component is also pronounced in the “310 nm” excitation experiment (Figure 3a): the 350 fs decay is in the latter case followed by a 6 ps rise thus causing a dip in the transient. The 0.35 ps decay component is well

within the experimental time resolution. (See also the discussion given below of the rise components in the transients detected at 460 and 620 nm as illustrated in Figure 4.) The 350 fs decay component is observed only at the shortest detection wavelength possible in the up-conversion experiment, i.e., at 460 nm. (The cutoff filter in the detection pathway prevents the detection of fluorescence at wavelengths shorter than 450 nm). This wavelength of 460 nm is at the trailing edge of the blue wing of the BP(OH)₂ band emission. In our previous experiments, detection at wavelengths shorter than 480 nm was not performed and the fast ~350 fs component remained unnoticed.^{8–11} Remark that when excitation is at 380 nm and detection is at 460 nm, the initial value of the fluorescence anisotropy attains the maximum value of 0.4 (Figure 2a). This value is the theoretically expected limiting value for the fluorescence anisotropy in case the electronic transition dipole moments for absorption and emission are oriented parallel to each other. Thus, an initial anisotropy of $r \cong 0.4$ is expected when the impulsively excited “di-enol” Franck–Condon state emits at 460 nm. From the relative positions and shapes of the steady-state absorption and emission spectra of BP(OH)₂ (Figure 1) it is highly likely that the “di-enol” Franck–Condon state would emit near 460 nm indeed. We thus propose that the ~350 fs component, which is most clearly observed when detecting the parallel polarized fluorescence transients at 460 nm, is due to BP(OH)₂ in the “di-enol” photoexcited state.

It is recalled that the decay rate of the “di-enol” excited state is determined by the formation rates of the “mono-” and “di-keto” initial products. These latter rates could previously not be determined from time-resolved experiments^{8,15} although they were estimated to be faster than (150 fs)⁻¹. The decay time of 350 fs of the “di-enol” state is close enough to the formation time of about 150 fs or less estimated previously for the initial “mono-” and “di-keto” tautomers to conclude that similar times are found for the decay of the “di-enol” and the formation of the “mono-” and “di-keto” tautomers. **Our present finding is therefore that the initial proton transfer is not only manifested as a very fast formation of the “mono-keto” and “di-keto” tautomer product states but also in the fluorescence decay of the initially excited “di-enol” state.**

When excitation is at 310 nm (keeping the detection at 460 nm), the initial fluorescence anisotropy is somewhat reduced ($r(0) \cong 0.3$, cf. inset Figure 3a). Probably competitive vibrational relaxation processes result in a (partial) loss of the contribution of the initially excited higher vibrational levels to the “di-enol” emission. These vibrational relaxation processes are very fast and probably involve IVR in analogy to several other chromophores of similar size.^{16,17,24} This result is in agreement with a similar conclusion obtained previously from the influence of the wavelength of the pump pulses on the yield of the “mono-keto” intermediate in the consecutive mechanism. In these experiments the “mono-keto” yield is always below its statistical limit value when the excitation photons are of higher energy. Most likely, at higher excitation energies for the “di-enol” tautomer, the formation of the “mono-keto” component has to compete with vibrational relaxation (IVR).⁹

Normally information about the lifetime of an emissive state is not contained in the time dependence of the fluorescence anisotropy. The reason is simply that for a Franck–Condon transition, the lifetime decay factor occurs in both the nominator and denominator of expression (1) and thus cancels out. However, in the case of BP(OH)₂ the proton transfer is considered to involve an ultrafast relaxation along an strongly asymmetric adiabatic potential energy surface (APES).¹⁰ Due

to the high anharmonicity of the excited-state potential energy surface, the diabatic states that could be designated as predominantly of “di-enol”, “mono-keto”, and “di-keto” character become mixed, the degree of mixing being dependent on proton-transfer reaction coordinates typical of the concerted and consecutive proton-transfer reactions. Thus, as the system relaxes along the potential energy surface, the electronic part of the wave function is modified and the transition dipole moment may be affected accordingly. Indeed, previous INDO/S calculations have indicated that the directions of the transition moments for the first excited states of the “mono-keto” and “di-keto” tautomers are almost parallel but different by about 13 degrees from that for the “di-enol” tautomer.⁵ In practice, the monitored fluorescence signal centered near a preselected detection wavelength comprises the fluorescence response of an ensemble of molecules for which the density distribution as a function of the reaction coordinate is inhomogeneously broadened. For the aforementioned reason, the transition dipole moments characteristic of the molecules in the ensemble will also exhibit inhomogeneity. At the preselected detection wavelength, the probed fluorescence is the integrated response of the inhomogeneous ensemble, within which the anisotropy is changing with time. It is for this reason that it is possible that the “di-enol” lifetime decay is reflected in its fluorescence anisotropy decay.

In view of the result that the decay of the “di-enol” Franck–Condon excited state could be resolved when detection is at 460 nm, we have reexamined the initial rise monitored at 620 nm, with special focus on the behavior in the narrow time window of 3 ps. Results for magic-angle transients are presented in Figure 4. The figure includes for comparison the rise component when detection is at 460 nm. It is clear that a distinct rise for the two transients is observed. Whereas the 460 nm component shows an instantaneous rise (within ~150 fs), as expected for the directly pumped “di-enol” emission, the 620 nm emission rises with a time of approximately 350 fs. Since the 620 nm emission contains contributions due to simultaneously formed “mono-keto” and “di-keto” tautomers,^{8,15} it follows that these components are formed with a typical time of 350 fs.

In discussing the ~350 fs decay component detected at 460 nm, the influence of the dynamic response of the environment to the optical excitation of the chromophore should also be considered.²⁵ Ultrashort solvation dynamics has been studied in numerous systems and has been found to include dynamics ranging from ~50 fs to several hundreds of picoseconds.^{26–28} Solvation has also been found to influence fluorescence anisotropy on a picosecond time scale.^{18,19} However, for BP(OH)₂, a solvent-polarity dependent Stokes shift could not be resolved.⁸ Fluorescence anisotropy dynamics caused by solvation is thus not likely. In summary, it is concluded that the kinetics for the excited-state decay of the “di-enol” tautomer and the formation of the “mono-” and “di-keto” tautomers in the emissive state have been observed. The results are compatible with an initial proton-transfer step with a typical time of 350 fs.

The time scale of about 350 fs for the initial proton-transfer steps is typical of a (quasi-) barrierless transition in which the system develops from the “di-enol” to the “mono-keto” and “di-keto” forms. Recall that, as discussed above, within the context of a (quasi-) barrierless excited-state relaxation it is assumed that the electronic wave function is gradually changing. Whereas usually a reaction is characterized by a probability for a transition between quasi-stable states, the initial proton-transfer reactions discussed here are visualized to involve a continuous

change of the excited-state electronic wave function. Low-frequency skeletal modes with a frequency near $250\text{--}350\text{ cm}^{-1}$ may promote the single and double-proton transfer in $\text{BP}(\text{OH})_2$. Such frequencies of skeletal modes of $\text{BP}(\text{OH})_2$ could indeed be measured from Raman measurements.²⁹ Furthermore, previously no deuteration effect could be observed for the double proton/deuteron transfer dynamics¹⁰ thus confirming that skeletal modes and not just single proton/deuteron particles are involved in the conformational changes.

Several decay components in the various fluorescence transients, at different detection wavelengths and polarizations, were obtained on a time scale of 10–100 picoseconds (cf Table 1). The “40 ps” decay component in the parallel-polarized fluorescence decay transient detected at 460 nm (Figure 3a) is characteristic of the effects of rotational diffusion of the $\text{BP}(\text{OH})_2$ molecules in cyclohexane. Assuming the Debye–Stokes–Einstein approximation, and taking $\eta = 0.89$, the effective radius, R , of the $\text{BP}(\text{OH})_2$ molecule, is calculated to be $R = 3.5\text{ \AA}$, which compares well with the van der Waals radius that is estimated as $R = 3.5\text{ \AA}$. Furthermore, we find that the characteristic time for this decay component is dependent on the nature of the solvent (e.g., approximately 25 ps in case the solvent is acetonitrile) and that this time becomes longer as the temperature is lowered.³⁰ These features are additional support that the 40 ps component is due to reorientational motions of the solute.

The perpendicular-polarized “460 nm” emission, obtained when excitation is at 380 nm, shows, following its preparation (55%), an additional rise with a typical time of about 12 ps (40%). In considering the latter kinetics, we recall that the emission detected at 460 nm is due to the “di-keto” tautomer formed in the concerted process and the “di-keto” species formed in the consecutive process. We may now consider the following contributions for the 12 ps perpendicular-polarized component. The perpendicular-polarized intensity due to the ultrafast “di-keto” component, increases with a time of ~ 40 ps because rotational diffusion motions lead to depolarization of the emission. The second component involves formation of the “di-keto” tautomer (and concomitant decay of the “mono-keto” tautomer) with a time of about 10 ps. The resulting kinetics is determined by the weighted average of the two contributions and may thus result in an effective rise time of about 12 ps.

As seen from Figure 2b, similar kinetics is obtained for the parallel and perpendicular polarized fluorescence transients detected at 620 nm (excitation is at 380 nm): the parallel component decays at a time of about 12 ps, while the perpendicular component shows a rise with a time of about 14 ps. The kinetics of the parallel-polarized emission is rationalized by taking into account that the “620 nm” emission is a combination of the fluorescence derived from the “mono-keto” intermediate and the instantaneously formed “di-keto” tautomer. The “mono-keto” species decays with a time of 10–12 ps. The net result of the two processes on the parallel-polarized emission intensity will thus depend on the details of the kinetics of the vibronic levels involved. The observed decay has a typical time (~ 12 ps) somewhat longer than the typical decay time of 10 ps for the “mono-keto” species. This slight difference may be rationalized by considering the contribution of the “di-keto” component produced in the concerted ESDPT process. This “di-keto” component causes an additional fluorescence decay component (with a time of about 40 ps), due to the reorientational diffusion motions of the solute. The overall time dependence of $I_{\parallel}(t)$ is then the weighted average of the two contributions considered here.

The time dependence of the perpendicular polarized “620 nm” transient (Figure 2b) is discussed in a similar way. We consider the “14 ps” intensity increase to result from contributions of “mono-keto” and “di-keto” excited-state dynamics. First, there is the competition between the ~ 10 ps decay of the “mono-keto” intermediate emission and the corresponding rise of the “di-keto” emission, both contributing to $I_{\perp}(t)$ at 620 nm. Since a rise is observed (with a time close to the proton-transfer time of 10 ps), we infer that now the intensity of the fluorescence decay of the “mono-keto” decay is weaker than the intensity rise due to the “di-keto” component. Furthermore, $I_{\perp}(t)$ will increase (with a time of ~ 40 ps) due to the rotational diffusion motions of the “di-keto” component that was already formed in the concerted mechanism. The overall intensity of $I_{\perp}(t)$ will be the weighted average of the aforementioned contributions and thus may result in the rise as observed, with a time of 14 ps.

From the time behavior of $I_{\parallel}(t)$ and $I_{\perp}(t)$, it immediately follows that the transient for the anisotropy parameter, $r(t)$, at the detection wavelength of 620 nm, decays with typical times of ~ 350 fs and 14 ps. The short time derives from the rapid rise component of $I_{\perp}(t)$, as discussed before (see also Figure 4). The 14 ps component is due to the disparity in the decay times of the parallel and perpendicular components and mainly reflects the effect of proton-transfer involved in the consecutive ESDPT. The maximum value of the anisotropy of the “620 nm” emission is 0.37 (insert Figure 2b). The presence of this anisotropy shows that appreciable fluorescence polarization is conserved during the initial excited-state proton transfer processes. It follows that the fluorescence anisotropy undergoes only a minor change when the “di-enol” tautomer decays into the “di-keto” and “mono-keto” tautomers indicating small directional changes among the transition dipole moments in these species. This finding is in support of the predictions of previous INDO/S calculations.⁵

As illustrated in Figure 3a, when excitation is at 310 nm, the parallel-polarized “460 nm” fluorescence transient initially displays a pronounced fast decay (~ 0.5 ps) representative of a fast process leading to a fluorescence intensity decrease. As discussed above for the “380 nm” excitation experiments, we attribute this very fast component to the Franck–Condon excited “di-enol” emission. Following the “0.5 ps” decay, the parallel-polarized emission shows an intensity *increase*. The typical time of this rise is about 6 ps. This rise component is evidence for the presence of a 6 ps excited-state feeding process for the “di-keto” tautomer, in addition to the ultrafast (~ 350 fs) “di-keto” tautomer formation. We attribute this feeding, as before, to the “mono-keto”-to-“di-keto” tautomer conversion, but now at a somewhat enhanced rate. The shortening from 10 to 6 ps of the “mono-keto” to “di-keto” reaction at higher photon excitation energies may indicate that the conversion may involve also vibrationally excited “mono-keto” tautomer species (proton transfer of “hot” molecules). Eventually, $I_{\parallel}(t)$ contains 40 ps and 3 ns decay components representative of the “di-keto” rotational diffusion and lifetime decay, respectively.

The perpendicular-polarized “460 nm” fluorescence transient, with excitation at 310 nm, also shows a small ~ 0.35 ps decay part, followed by a rise with a typical time of about 14 ps. The ~ 0.35 ps component is again attributed to the rapid initial “di-enol” emission decay mentioned above. The “14 ps” rise contains, as before, several contributions. One contribution arises from the feeding of the “di-keto” tautomer (in the consecutive reaction) and the second part is due to rotational diffusion motions of the “instantaneously” formed “di-keto” tautomer.

The overall intensity increase with an effective time of about 14 ps is, as before, the weighted average of the two contributions.

The time dependence of the "460 nm" fluorescence anisotropy is readily rationalized by combining the individual effects of $I_{\parallel}(t)$ and $I_{\perp}(t)$. The anisotropy is found to exhibit initially the ~ 0.35 ps component due to the "di-enol" emission. This component is followed by the dominant part with a time constant of about ~ 18 ps. This decay is attributed to the combined effects of "mono-keto" to "di-keto" dynamics (~ 6 ps) as well as the rotational diffusion (~ 40 ps) of the "di-keto" species.

The initial value of the anisotropy of the "620 nm" emission is about 0.3 (Figure 3 b, insert). Excitation at 310 nm is likely to enhance the influence of proton transfer from higher vibrational levels (vide supra) and this may lead to an initial fluorescence anisotropy lower than when excitation is at 380 nm. Faster decay kinetics of the fluorescence transients at 310 nm excitation is also illustrated in the parallel-polarized transient of the "620 nm" emission (Figure 3 b). Initially, a "7 ps" decay component is found that should be compared with the "12 ps" decay when excitation is at 380 nm. The 7 ps decay is attributed to the "mono-keto" to "di-keto" reaction, but now at a higher rate because for the higher vibrational states apparently the "mono-keto" to "di-keto" reaction is faster. The perpendicular-polarized "620 nm" fluorescence transient is characterized by a 40 ps rise component followed by the 3 ns lifetime decay. As before, the 40 ps rise originates from the rotational diffusion motions of the "di-keto" tautomer (see discussion of the 380 nm excitation experiments).

The "620 nm" anisotropy decay curve obtained when excitation is at 310 nm is multiexponential containing short characteristic times of 0.35 and 3 ps and a longer time of 18 ps. The short times derive from the growth of the "mono-keto" component, whereas the 18 ps component is attributed to the combined effects of "mono-keto" to "di-keto" dynamics (~ 6 ps) as well as the rotational diffusion (~ 40 ps) of the "di-keto" species.

The results obtained for BP(OH)₂ dissolved in acetonitrile are summarized in Table 2. When detection is at 460 nm, a short decay component was found in the time-resolved fluorescence of BP(OH)₂, although the decay now looks somewhat shorter (~ 0.2 – 0.3 ps). Again, this component is attributed to the emissive decay of the initially excited "di-enol" Franck–Condon state. Additionally, components due to rotational diffusion and lifetime decay are found, both in the polarized transients and the fluorescence anisotropy. The fluorescence anisotropy now contains three decay components, with time constants of approximately 0.25, 10, and 20 ps. These times are somewhat shorter than the time of 40 ps found for the rotational diffusion motions in the cyclohexane liquid. We attribute the 10 and 20 ps components to the rotational diffusion motions in the acetonitrile liquid, although it remains unclear why in the latter solvent these motions are characterized by two (instead of one) exponential terms. The lifetime of the fluorescent state of BP(OH)₂ is somewhat solvent dependent: 1 ns in acetonitrile, 3 ns when the solvent is cyclohexane. In summary, the gross features in acetonitrile and cyclohexane remain similar, and thus a detailed discussion as given above for BP(OH)₂ in cyclohexane, is not repeated here for BP(OH)₂ in acetonitrile.

5. Conclusion

A fast decay component, with a characteristic time of ~ 350 fs, is observed when detection is at 460 nm, i.e., at the tail of the blue side of the broad-band emission of BP(OH)₂ in

cyclohexane (the decay is somewhat shorter in acetonitrile). The fast fluorescence decay is not observed when detection is above 480 nm. The short-living emission is assigned to the Franck–Condon excited state of the "di-enol" tautomer. The "di-enol" excited state is the initial state in a branched excited-state double proton-transfer process in which the products are excited-state "mono-keto" and "di-keto" tautomers. The typical formation times of these "keto" molecules are compatible with the decay kinetics of the "di-enol" species, thus providing independent additional support for the ESDPT model proposed previously.⁸ The ~ 350 fs decay also appears in the fluorescence anisotropy decay of BP(OH)₂. This is a direct consequence of the (quasi-) barrierless nature of the excited-state APES as a function of the reaction coordinate. This APES gives rise to a strong mixing of the diabatic wave functions characteristic of the tautomeric forms, thus the electronic wave function, and concomitantly the direction of the transition dipole, become sensitively dependent on the reaction coordinate. Since experimentally we probe the temporal behavior of the fluorescence of molecules within a narrow window of the proton transfer reaction coordinate, the fluorescence anisotropy closely reflects the excited-state relaxation along the APES. Finally, the fluorescence anisotropy decay kinetics also reflects decay components with time constants of a few tens of picoseconds. These components are representative of the influence of the consecutive double-proton transfer and rotational diffusion motions of the solute molecules in the liquid.

References and Notes

- (1) (a) Agmon, N.; Gutman, M., Eds. *Isr. J. Chem.* **1999**, 39 (3/4) (*Proton Solvation and Proton Mobility*, special issue). (b) Limbach, H.; Manz, J., Eds. *Ber. Bunsen-Ges. Phys. Chem.* **1998**, 102 (*Hydrogen Transfer: Experiment and Theory*, special issue). (c) Perrin, C. L.; Nielson, J. B. *Annu. Rev. Phys. Chem.* **1997**, 48, 511.
- (2) See, e.g.: (a) Douhal, A.; Lahmani, F.; Zewail, A. H. *Chem. Phys.* **1996**, 207, 477. (b) Ameer-Beg, S.; Ormson, S. M.; Brown, R. G.; Matousek, P.; Towrie, M.; Nibbering, E. T. J.; Fogg, P.; Neuwahl, F. V. R. *J. Phys. Chem. A* **2001**, 105, 3709. (c) Ernsting, N. P.; Kovalenko, S. A.; Senyushkina, T.; Saam, J.; Farztdinov, V. *J. Phys. Chem. A* **2001**, 105, 3443. (d) Fournier, T.; Pommeret, S.; Mialocq, J. C.; Deflandre, A.; Rozot, R. *Chem. Phys. Lett.* **2000**, 325, 171. (e) Fiebig, T.; Chachisvilis, M.; Manger, M.; Zewail, A. H.; Douhal, A.; Garcia-Ochoa, I.; Ayuso, A. D. H. *J. Phys. Chem. A* **1999**, 103, 7419. (f) Chudoba, C.; Riedle, E.; Pfeiffer, M.; Elsaesser, T. *Chem. Phys. Lett.* **1996**, 263, 622. (g) Lochbrunner, S.; Wurzer, A. J.; Riedle, E. *J. Chem. Phys.* **2000**, 112, 10669. (h) Glasbeek, M. *Isr. J. Chem.* **1999**, 39, 301. (i) Chou, P. T.; Wu, G. R.; Wei, C. Y.; Shiao, M. Y.; Liu, Y. I. *J. Phys. Chem. A* **2000**, 104, 8863.
- (3) Sepiol, J.; Bulska, H.; Grabowska, A. *Chem. Phys. Lett.* **1987**, 140, 607.
- (4) Kaczmarek, L.; Borowicz, P.; Grabowska, A. *J. Photochem. Photobiol. A: Chem.* **2001**, 138, 159.
- (5) Bulska, H. *Chem. Phys. Lett.* **1983**, 98, 398.
- (6) Wortmann, R.; Elich, K.; Lebus, S.; Liptay, W.; Borowicz, P.; Grabowska, A. *J. Phys. Chem.* **1992**, 96, 9724.
- (7) Borowicz, P.; Grabowska, A.; Wortmann, R.; Liptay, W. *J. Lumin.* **1992**, 52, 265.
- (8) Zhang, H.; van der Meulen, P.; Glasbeek, M. *Chem. Phys. Lett.* **1996**, 253, 97.
- (9) Marks, D.; Proposito, P.; Zhang, H.; Glasbeek, M. *Chem. Phys. Lett.* **1998**, 289, 535.
- (10) Marks, D.; Zhang, H.; Glasbeek, M.; Borowicz, P.; Grabowska, A. *Chem. Phys. Lett.* **1997**, 275, 370.
- (11) Proposito, P.; Marks, D.; Zhang, H.; Glasbeek, M. *J. Phys. Chem. A* **1998**, 102, 8894.
- (12) Barone, V.; Adamo, C. *Chem. Phys. Lett.* **1995**, 241, 1.
- (13) Sobolewski, A. L.; Adamowicz, L. *Chem. Phys. Lett.* **1996**, 252, 33.
- (14) Strictly speaking a "di-keto" mesomeric structure for BP(OH)₂ does not exist. However, we follow the convention in the literature for BP(OH)₂ and still designate its double-proton-transfer form as the "di-keto" tautomer.
- (15) Neuwahl, F. V. R.; Fogg, P.; Brown, R. G. *Chem. Phys. Lett.* **2000**, 319, 157.
- (16) Arzhantsev, S. Y.; Takeuchi, S.; Tahara, T. *Chem. Phys. Lett.* **2000**, 330, 83.
- (17) Chou, P. T.; Chen, Y. C.; Yu, W. S.; Chou, Y. H.; Wei, C. Y.; Cheng, Y. M. *J. Phys. Chem. A* **2001**, 105, 1731.

- (18) van Veldhoven, E.; Zhang, H.; Glasbeek, M. *J. Phys. Chem. A* **2001**, *105*, 1687.
- (19) Sarkar, N.; Takeuchi, S.; Tahara, T. *J. Phys. Chem. A* **1999**, *103*, 4808.
- (20) Yeh, A. T.; Shank, C. V.; McCusker, J. K. *Science* **2000**, *289*, 935.
- (21) Lakowicz, J. R. *Principles of Fluorescence Spectroscopy*, 2nd ed.; Plenum: New York, 1999.
- (22) Middelhoek, E. R.; van der Meulen, P.; Verhoeven, J. W.; Glasbeek, M. *Chem. Phys.* **1995**, *198*, 573.
- (23) Bulska, H.; Grabowska, A.; Grabowski, Z. R. *J. Lumin.* **1986**, *35*, 189.
- (24) De Belder, G.; Schweitzer, G.; Jordens, S.; Lor, M.; Mitra, S.; Hofkens, J.; De Feyter, S.; Van der Auweraer, M.; Hermann, A.; Weil, T.; Müllen, K.; De Schryver, F. C. *ChemPhysChem.* **2001**, *1*, 49.
- (25) Bagchi, B.; Biswas, R. *Adv. Chem. Phys.* **1999**, *109*, 207.
- (26) (a) Jimenez, R.; Fleming, G. R.; Kumar, P. V. Maroncelli, M. *Nature* **1994**, *369*, 471. (b) Horng, M. L.; Gardecki, J. A.; Papazyan, A.; Maroncelli, M. *J. Phys. Chem.* **1995**, *99*, 17311.
- (27) (a) Zhang, H.; Jonkman, A. M.; van der Meulen, P.; Glasbeek, M. *Chem. Phys. Lett.* **1994**, *224*, 551. (b) van der Meulen, P.; Zhang, H.; Jonkman, A. M.; Glasbeek, M. *J. Phys. Chem.* **1996**, *100*, 5367.
- (28) Kovalenko, S. A.; Ernsting, N. P.; Ruthmann, J. *J. Chem. Phys.* **1997**, *106*, 3504.
- (29) Borowicz, P.; Faurskov-Nielsen, O.; Christensen, D. H.; Adamowicz, L.; Les, A.; Waluk, J. *Spectrochim. Acta A* **1998**, *54*, 1291.
- (30) Toele, P.; Zhang, H.; Glasbeek, M. Unpublished results.